Ahmad Rafiee[1]
Mehdi Panahi[2]

[1]Sharif Engineering Process Development Company (SEPDCO), Tehran, Iran.

[2]Chemical Engineering Department, Faculty of Engineering, Ferdowsi University of Mashhad, Mashhad, Iran.

Optimal Design of a Gas-to-Liquids Process with a Staged Fischer-Tropsch Reactor

The optimal design of a natural gas-to-liquid hydrocarbons (GTL) process with a multistage cobalt-based Fischer-Tropsch reactor and interstage product separation is considered. The objective function is to maximize the wax (C_{21+}) production rate at the end of the reactor path. Sectioning of the Fischer-Tropsch reactor increases the chain growth probability inside the reactor which results in a higher production of wax. The carbon efficiency of the two-stage reactor is distinctly higher than that of the single-stage reactor.

Keywords: Fischer-Tropsch synthesis, Gas-to-liquid process, Reactor staging, Wax production

Received: January 21, 2016; *revised:* March 19, 2016; *accepted:* May 20, 2016

DOI: 10.1002/ceat.201600040

1 Introduction

Fischer-Tropsch synthesis (FTS) was first described in the literature in 1935 [1]. FTS became increasingly attractive due to the recent developments and improvements of the technology, clean-burning fuels derived from the process (low sulfur, low aromatics), and because the process can be used to convert natural gas resources in remote areas to transportable liquid fuels.

In the Fischer-Tropsch reactor, the synthesis gas (syngas) containing mainly H_2 and CO is converted to a wide range of hydrocarbons like paraffins, olefins, oxygenates etc., and then upgraded to intermediate or final fuels and chemicals [2]. Any rich carbon raw material may be used as feedstock to produce syngas. The type of the feedstock, e.g., biomass, coal or natural gas, will determine the technology of the syngas production section [3]. When coal or biomass is employed as raw feed, the syngas is produced by gasification.

There are several routes to produce syngas from natural gas, i.e., auto-thermal reforming (ATR), steam methane reforming (SMR), combined reforming, and gas-heated reforming (GHR) [1]. For gas-to-liquid (GTL) applications, it is claimed that the ATR is the most economical technology to produce syngas [4, 5].

Iron or cobalt catalysts are mainly used in the FT reactor [6]. Water-gas shift reaction is active on iron catalysts but negligible on cobalt catalysts. Four different types of reactors are used to convert syngas to liquid fuels: fixed-bed, slurry bubble column, fluidized-bed, and circulating fluidized-bed reactors [1]. The product distribution in the FT reactor depends on the composition of syngas, operating conditions, FT catalyst type, reactor technology employed for FT synthesis, and deactivation of FT catalyst [1]. The raw product leaving the FT reactor is sent to an upgrading section for further treatment in order to meet the final product specifications (Fig. 1) [2].

Syngas production and upgrading of FT products are already established and developed technologies, e.g., syngas production is widely used in methanol and ammonia synthesis and upgrading of FT products originates from the petroleum refining industry. The FT synthesis could be optimized and developed in different ways to reduce the investment cost and, in addition, there is a need to improve carbon and energy efficiencies.

The Sasol Oryx GTL plant in Qatar is the world's first commercial-scale GTL plant with a production capacity of 34 000 bbl day^{-1} liquid fuels. There are two parallel trains with two cobalt-based slurry bubble column reactors (SBCR). The volume of each reactor is 2000 m^3 [7].

The largest operating GTL plant is the Shell Pearl plant in Qatar with a production capacity of 260 000 bbl day^{-1}: 120 000 bbl day^{-1} upstream products and 140 000 bbl day^{-1} GTL products. There are two parallel trains in this plant and the proprietary Shell middle distillate synthesis (SMDS) process is applied. Methane and oxygen from the air separation unit (ASU) are converted into syngas. Syngas is then cooled down to produce steam via the steam turbines. In the next stage, the syngas passes through 24 fixed-bed reactors filled with Shell proprietary cobalt synthesis catalyst inside the tubes. Syngas is converted into very heavy and waxy hydrocarbons and water in the FT reactors. In the upgrading section, the wax from the FT reactors is hydrocracked into shorter chains and in a distillation column the hydrocracked cuts are separated [8].

This study is the continuation of our previous work where auto-thermal reforming (ATR) is used to convert natural gas to syngas. The kinetic model for FT reactions is the one given by Iglesia et al. for a cobalt-based FT reactor [9]. The overall process flow sheet is presented in Fig. 2 [9] which is used to study the sectioning of the FT reactor. In all cases, the total volume is fixed at 2000 m^3, i.e., the same volume of the Sasol Oryx slurry

Correspondence: Dr. Mehdi Panahi (mehdi.panahi@um.ac.ir), Chemical Engineering Department, Faculty of Engineering, Ferdowsi University of Mashhad, Mashhad, Iran.

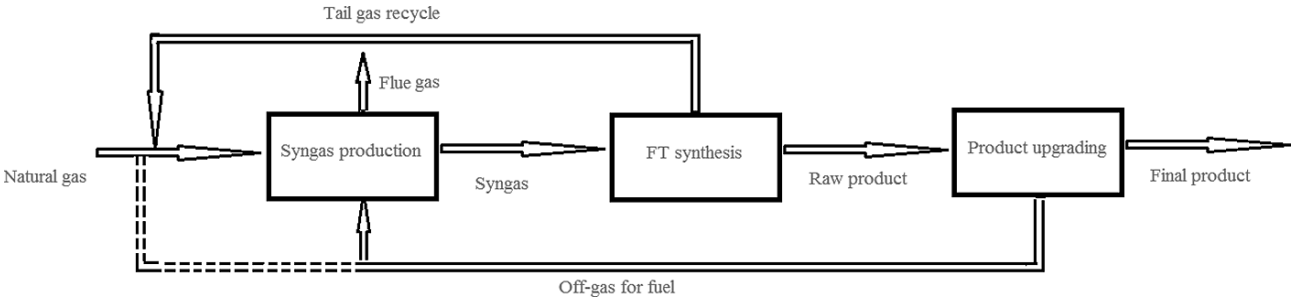

Figure 1. Simple process flow diagram of a GTL process [2].

reactor. Staging of the FT reactor will provide more degrees of freedom for optimization.

Sectioning of chemical reactors into stages has been widely applied. Androulakis and Reyes investigated oxidative coupling of methane (OCM) on a multistage plug-flow reactor [10]. The effect of feed distribution in a packed-bed membrane reactor for methanol oxidative dehydrogenation was studied by Diakov and Varma [11]. Conversion of a staged slurry bubble column reactor for FTS was optimized by Maretto and Krishna [12]. Oxygen distribution and selective combustion of hydrogen during propane dehydrocyclodimerization reactions was performed by Waku et al. [13]. The effect of catalyst dilution and feed distribution of two case studies involving nitrobenzene hydrogenation and ethylene oxidation was investigated by Hwang and Smith [14]. Guillou et al. [15] studied the effect of distributed hydrogen in a microchannel FT reactor.

The effect of main operating variables such as temperature, partial pressure of hydrogen, liquid and hydrogen flow rates on conversion of hydrogen and selectivity of cyclo-dodecene in consecutive hydrogenation of 1,5,9-cyclododecatriene to cyclo-dodecene was analyzed by Stuber and Delmas [16] in a multistage operation. Ngwenya et al. [17] examined the influence of operating parameters on the performance of the cobalt catalyst-based FT reactor with different objective functions. Manenti et al. investigated possible design improvement in a series of fixed-bed reactors for methanol and dimethyl ether synthesis [18]. Hillestad applied the systematic staging method on a methanol reactor [19]. Staging will increase the production rate of methanol at the end of the reactor path. Staging of the FT reactor individually (single pass) was recently published for iron- and cobalt-based catalysts. A lumping technique was used to reduce the number

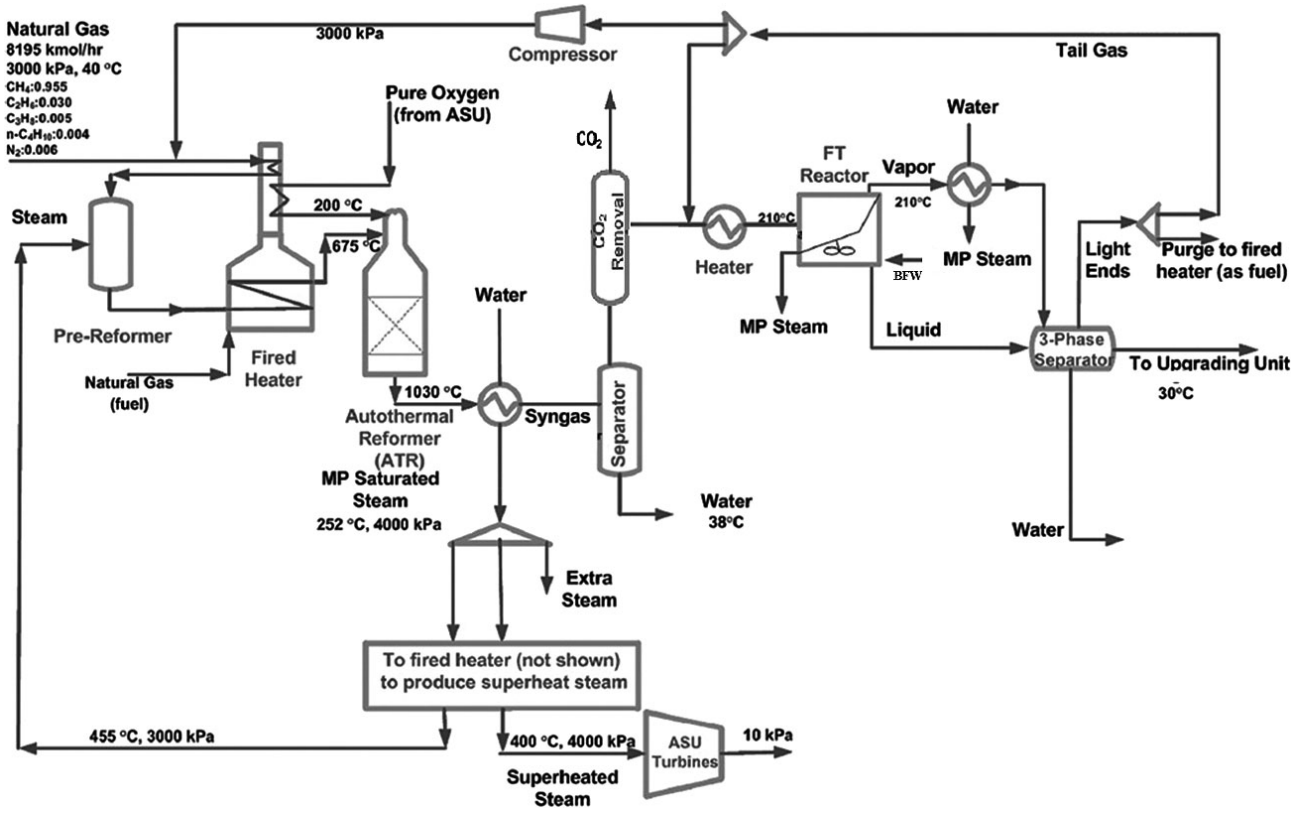

Figure 2. Scheme of a GTL plant [9].

of components. Staging of the FT reactor will increase the production rate of key components [20, 21].

2 Modeling and Process Description

2.1 Synthesis Gas (Syngas) Production

The syngas step converts the natural gas feed into a mixture containing mainly H_2 and CO. The key variable is the H_2/CO ratio at the outlet of the syngas unit. The optimal H_2/CO ratio depends on the FT technology. Although a usage ratio of 2:1 is implied by the FT reactions, the real usage ratio depends on the chain growth probability and product selectivity.

Natural gas feed is preheated and then fed to the prereformer to have full conversion of higher hydrocarbons than methane to H_2 and CO. In addition, the methanation and water-gas shift reactions are assumed to be in equilibrium [4, 22].

$$C_nH_m + nH_2O \rightarrow nCO + (n + m/2)H_2 \quad (1)$$

The stream leaving the prereformer is further heated and then goes through the auto-thermal reformer (ATR).

The most important reactions in the ATR are listed below [23]:

$$CH_4 + 1.5O_2 \rightleftharpoons CO + 2H_2O \qquad \Delta H^0_{298} = -520\,\text{kJ mol}^{-1} \quad (2)$$

$$CH_4 + H_2O \rightleftharpoons CO + 3H_2 \qquad \Delta H^0_{298} = 206\,\text{kJ mol}^{-1} \quad (3)$$

$$CO + H_2O \rightleftharpoons CO_2 + H_2 \qquad \Delta H^0_{298} = -41\,\text{kJ mol}^{-1} \quad (4)$$

In this study, chemical equilibrium at the ATR outlet is assumed which is a reasonable assumption for simulation purposes.

2.2 Fischer-Tropsch Synthesis

In the FT reactor, the syngas reacts to form a mixture of hydrocarbons with different chain length [24].

$$CO + U_{H2}H_2 \rightarrow -CH_2- + H_2O \quad (5)$$

where U_{H2}[1)] is the usage ratio of H_2. The kinetic model applied in this study is the one given by Iglesia et al. for a cobalt catalyst, where methane production and CO consumption are given by Eqs. (6) and (7), respectively [25].

$$r_{CH_4} = \frac{k_1 P_{H_2} P_{CO}^{0.05}}{1 + K_1 P_{CO}} \quad (6)$$

Table 1. Kinetic and adsorption parameters in Eqs. (6) and (7) [9].

Parameter	Arrhenius expression
k_1 [$\text{kmol}_{CH4}\text{Pa}^{-1.05}\,\text{m}^{-3}_{\text{reactor}}\text{s}^{-1}$]	$8.8\times10^{-6}\exp(-\frac{37326}{RT})$
K_1 [Pa^{-1}]	$1.096\times10^{-12}\exp(-\frac{-68401.5}{RT})$
k_2 [$\text{kmol}_{CO}\text{Pa}^{-1.25}\,\text{m}^{-3}_{\text{reactor}}\text{s}^{-1}$]	$1.6\times10^{-5}\exp(-\frac{37326}{RT})$

$$r_{CO} = \frac{k_2 P_{H_2}^{0.6} P_{CO}^{0.65}}{1 + K_1 P_{CO}} \quad (7)$$

Iglesia's reaction rate on a cobalt catalyst is valid at 473–483 K, 100–3000 kPa, H_2/CO = 1–10, and CO conversions lower than 15 %. It is assumed that this kinetic model is still valid for H_2/CO < 1 and CO conversion > 15 %. It is known that applying Iglesia's kinetic model outside the validity range is a possible source of error. This kinetic model is chosen because it takes into account a higher selectivity of methane. However, other available kinetic models could be applied, e.g., the kinetic model developed by Yates and Satterfield [24]. In their kinetic model, the consumption rate is measured in a well-mixed continuous-flow slurry reactor operating at T = 220–240 °C, P = 0.5–1.5 MPa, H_2/CO of feed = 1.5–3.5, conversion of H_2 and CO 6–68 % and 11–73 %, respectively. The mass fractions of FT products heavier than methane are assumed to follow an ideal Anderson-Schulz-Flory (ASF) distribution where α is the chain growth probability. For cobalt catalysts, chain growth probabilities between 0.85 and 0.95 are reported [26].

$$W_n = n(1-\alpha)^2\alpha^{n-1} \qquad n = 2, 3, \ldots, \infty \quad (8)$$

The carbon mass balance and production rates of paraffins and olefins as given by the ASF distribution model are presented in detail in our previous paper [9]. Three different methods for obtaining chain growth probability (α) are considered. For each carbon number, olefins and paraffins are produced, and the factor γ determines the olefins/paraffins ratio. This ratio is assumed to be constant and is equal to 0.35.

This study is based on the assumption that the FT reactor is a slurry bubble column-type reactor. The fluid mixing inside the reactor depends on the arrangement of the cooling tubes, superficial velocity of gas and liquid, geometry of the reactor, etc. In slurry reactors, the gas phase can be assumed to be plug flow while the liquid phase is suggested to be well-mixed. The reactions take place in the slurry phase. Here, the FT reactor is approximated with a continuous stirred-tank reactor (CSTR) operating at 210 °C [9]. The partial pressures of H_2 and CO inside the reactor are used to calculate the probability of chain growth. The pressure of syngas to the first reactor is 2459 kPa. A pressure drop of 2 bar along the reactor path is assumed. For a four-stage configuration, the pressure drop of each reactor is 50 kPa.

1) List of symbols at the end of the paper.

3 Results and Discussion

The FT reactor is sectioned into stages (n_s) and design functions are optimized to maximize an objective function. The objective function is maximization of wax production at the end of the reactor path. The degrees of freedom are: steam-to-hydrocarbon ratio (S/C) to the prereformer, oxygen-to-hydrocarbon ratio (O/C) to the ATR, purge ratio, the recycled tail gas fraction to the syngas and FT sections, CO_2 removal fraction, and number of stages.

In all cases, the total volume is fixed at 2000 m^3 which is equal to the volume of the Sasol slurry reactor at Oryx GTL plant in Qatar. Water and liquid hydrocarbons are separated by an interstage three-phase separator as depicted in Fig. 3.

An Aspen HYSYS process simulator is used to simulate and optimize the GTL process (Fig. 2) with a staged FT reactor (Fig. 3).

3.1 Case with Single-Stage FT Reactor (Base Case)

The base case is the GTL process with a single-stage FT reactor (n_s = 1), Fig. 2. The volume of the reactor is 2000 m^3. The optimization results of the base case are given in Tab. 2. The carbon efficiency in Tab. 2 is defined as the ratio of carbon moles in the final FT products and carbon moles in the feed to the process, including make-up natural gas used as fuel in the fired heater.

In the simulations, the fired heater duty is calculated to supply energy for the following streams [9]:

(a) Preheating the two streams below 455 °C:
  – fresh natural gas feed
  – recycled tail gas from the separator located downstream of the FT reactor (prereformer feed).
(b) Superheated steam as prereformer feed and superheated steam for driving the turbines of compressors in the ASU and also the recycled tail gas compressor.
(c) Preheating the ATR feed to 675 °C.
(d) Preheating the oxygen stream coming from the ASU to 200 °C.
(e) It is assumed that 10 % of the total fired heater duty are used to supply superheated steam for other mechanical and rotating equipment in the process.

In this case, the steam-to-carbon ratio to the prereformer and tail gas purge ratio become active in the provided lower bound of 0.4 % and 1 %, respectively. The temperature of the syngas leaving the ATR is always kept constant at 1030 °C by changing the amount of pure oxygen [9]. The H_2/CO ratio of fresh syngas is 0.73 and it is reduced to 0.52 when it is mixed with 61 % of the tail gas recycled to the FT reactor. The H_2/CO inside the reactor is 0.33. The probability of chain growth in this case is 0.966. The production rate of C_{21+} is 77753 kg h^{-1}. The amount of pure oxygen to adjust the outlet temperature of the ATR at 1030 °C is 6818 kmol h^{-1}. The ratio of recycled stream to the fresh syngas is 1.22 kg kg^{-1}. The flow rate of purge stream is 892 kmol h^{-1} and contains mainly CO (62.13 %), H_2 (20.50 %), CO_2 (9.19 %), and CH_4 (2.43 %). In the CO_2 removal unit, 1530 kmol h^{-1} of CO_2 is removed from the fresh syngas. The flow rate of syngas to the reactor is 109 500 kmol h^{-1}.

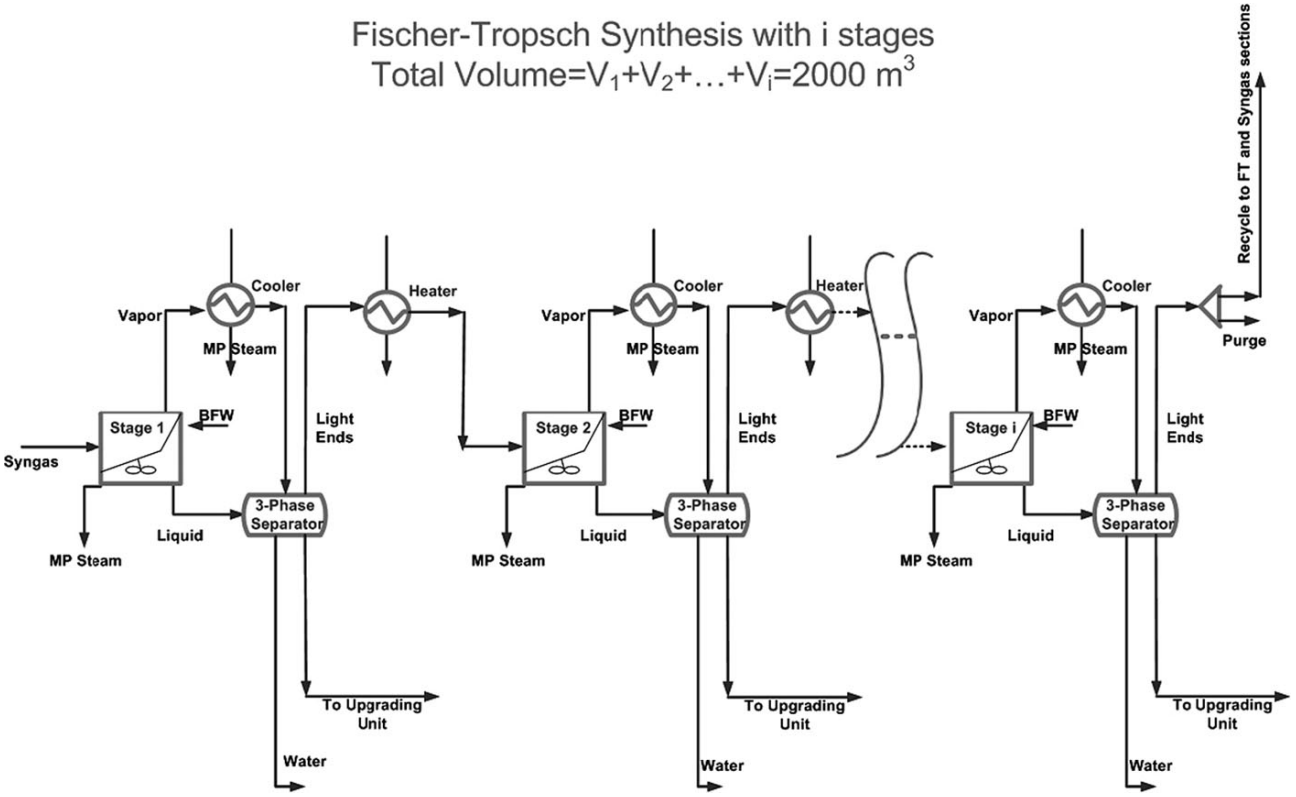

Figure 3. Multistage FT reactor with interstage product separation.

Table 2. Optimal design of the GTL process with different numbers of stages of the FT reactors.

	Single-stage	Two-stage	Three-stage	Four-stage
V_i of each stage [m^3]	2000	1000	666.67	500
H_2O/C [–]	0.4	0.4	0.4	0.4
O_2/C [–]	0.60	0.59	0.58	0.58
CO_2 removal [%]	32	25.61	26	26
Purge [%]	1	1	1	1
Recycle to FT [%]	61	80	80.70	80.70
H_2/CO fresh [–]	0.73	0.83	0.85	0.86
H_2/CO into FT/first reactor [–]	0.52	0.45	0.44	0.44
H_2/CO inside FT [–]	0.33	Reactor 1: 0.37	Reactor 1: 0.39	Reactor 1: 0.40
		Reactor 2: 0.30	Reactor 2: 0.34	Reactor 2: 0.36
			Reactor 3: 0.29	Reactor 3: 0.32
				Reactor 4: 0.29
α [–]	0.966	Reactor 1: 0.959	Reactor 1: 0.9566	Reactor 1: 0.9555
		Reactor 2: 0.970	Reactor 2: 0.9642	Reactor 2: 0.9613
			Reactor 3: 0.9721	Reactor 3: 0.9672
				Reactor 4: 0.9733
Carbon efficiency [–]	0.6241	0.6600	0.6673	0.6687
C_{21+} production rate [$kg\,h^{-1}$]	77 753	78 948	79 216	79 346

The total productions of methane and water in the FT reactor are 140 and 6689 $kmol\,h^{-1}$, respectively. The per pass conversions of H_2 and CO in the FT reactor are 42.97 and 10.78 %, respectively. On the other hand, the total conversions of H_2 and CO are 65.48 % and 23.21 %, respectively. The amount of heat needed to be removed from the FT reactor is 1.08×10^9 kJ hr^{-1}. The flow rate of make-up natural gas as fuel to the fired heater is 1620 $kmol\,h^{-1}$. In this case, 90 $kmol\,h^{-1}$ of CO_2 is emitted to the atmosphere via purge stream.

Tab. 3 summarizes the production rates of hydrocarbons inside the FT reactor (α = 0.966). From this table it can be seen that the selectivity of methane using the Iglesia's kinetic model is higher than for the case where the methane production rate follows the ASF model.

3.2 Case with Two-Stage FT Reactors and Product Separation between Stages

In this case, the GTL process with two FT reactors with equal volume is considered (n_s = 2). The stream leaving the first reactor is going through a three-phase separator to separate light gases, liquid hydrocarbon phase, and water. The light gases are sent to the second FT reactor. The effluent of the second FT reactor is sent to another three-phase separator to separate light gases, liquid hydrocarbon phase, and water. A part of the light gases from the second separator is purged and the rest is recycled back to the FT and syngas sections to increase the conversion of species.

The results of optimization of this case are presented in Tab. 2. Here, the CO_2 recovery percentage is lower than case 1 and the amount of tail gas recycled to the FT section is 80 % which is higher than case 1. The probabilities of chain growth inside the FT reactors are 0.959 and 0.970, respectively. Staging of the FT reactor increases the production of C_{21+} by 1.5 % compared to case 1. The amount of pure oxygen to adjust the outlet temperature of the ATR at 1030 °C is 6312 $kmol\,h^{-1}$ which is 506 $kmol\,h^{-1}$ (7.42 %) lower than case 1. The flow rate of the purge stream is 1236 $kmol\,h^{-1}$ and contains mainly CO (62.4 %), H_2 (18.9 %), CO_2 (11.1 %), and CH_4 (3.4 %). In the CO_2 removal unit, 984 $kmol\,h^{-1}$ of CO_2 is removed from the fresh syngas which is 546 $kmol\,h^{-1}$ (35.69 %) less than case 1. The flow rates of syngas to the first and second reactors are 144 700 and 133 500 $kmol\,h^{-1}$, respectively.

Table 3. Production rate of hydrocarbons inside the FT reactor (single-stage reactor).

Selectivity [%]	C_1	C_2	C_3–C_4	C_5–C_{10}	C_{11}–C_{20}	C_{21+}
Iglesia kinetic model (Eqs. (6) and (7))	2.37	0.22	0.72	4.02	10.49	82.18
Ideal ASF model (n = 1,2,…)	0.12	0.22	0.74	4.11	10.70	84.11

Conversions of H_2 in the first and second reactor are 20.01 % and 22.45 %, respectively, while the overall conversion of H_2 is 74.7 %. Per pass and overall conversions of CO are 8.43 % and 30.17 %, respectively. About 50.7 % of the wax is produced in the first FT reactor. In both reactors 6934 kmol h^{-1} of water is produced. The amount of heat needed to be removed from the first and second reactors to keep the reactor temperatures constant at 210 °C is 5.92×10^8 and 5.29×10^8 kJ h^{-1}, respectively. The amount of make-up natural gas to the fired heater is 1365 kmol h^{-1} which is 255 kmol h^{-1} lower than case 1. In this case, 148 kmol h^{-1} of CO_2 is emitted to the atmosphere via purge stream. The carbon efficiency of the two-stage reactor is 5.8 % higher than for the single-stage reactor.

The flow of oxygen from the air separation unit (ASU), CO_2 removal percentage, and amount of make-up natural gas as fuel to the fired heater is less than in the case with the single-stage reactor. These items will reduce the investment and operating costs of the plant. The production rate of wax is higher than for case 1, leading to higher carbon efficiency compared to case 1. On the other hand, staging provides more degrees of freedom for optimization and reduces the size and weight of each stage. A multistage reactor configuration facilitates maintenance, catalyst replacement, and introducing interstage feeding between the reactors. A multistage reactor will increase the process complexity in terms of multiple separation unit operations, utility requirements, control systems etc. and there is a trade-off between these factors.

As described earlier, Iglesia's reaction rate on cobalt catalysts is valid at CO conversions lower than 15 %. Using Iglesia's kinetic model outside the range of its validity is a possible source of error. The model used to determine the probability of chain growth (α) inside the FT reactor and also distribution of products according to the ideal ASF model are further sources of error. This is due to the fact that in reality the product distribution deviates from the ideal ASF model. High values of α in the optimal cases are due to the low H_2/CO ratios inside the FT reactor. It is known that using the α model outside the validity ranges of (H_2/CO) affects the product distribution. Using a constant olefin-to-paraffin ratio of 0.35 for all carbon numbers can be considered as another source of error. Approximating the slurry bubble column reactor as a CSTR affects the conversion of CO and H_2 and consequently the distribution of final products. The assumptions and simplifications made here have the same impact on all cases. The relative change of the wax production rate is important.

3.3 Case with Three-Stage FT Reactors and Product Separation between Stages

In this case, the GTL process with three-stage FT reactors is optimized (n_s = 3). A part of the light gases from the third three-phase separator is purged and the rest is recycled back to the FT and syngas sections.

The results of optimization are given in Tab. 2, being very close to the case with two-stage reactor. Staging of the FT reactor will increase the production of C_{21+} by 0.34 % compared to case 2 and there is not much to gain by having three stages. The amount of pure oxygen to adjust the outlet temperature of the ATR at 1030 °C is 6240 kmol h^{-1} which is 578 kmol h^{-1} less than in case 1. The ratio of recycled stream to the fresh syngas is 2.89 kg kg^{-1}. The flow rate of the purge stream is 1201 kmol h^{-1} and contains mainly CO (62.47 %), H_2 (18.25 %), CO_2 (11.15 %), and CH_4 (3.68 %). In the CO_2 removal unit, 952 kmol h^{-1} of CO_2 is removed from the fresh syngas, being 578 kmol h^{-1} less than in case 1. The flow rate of syngas to the first reactor is 141 400 kmol h^{-1}. The total production of methane in the reactors is 205 kmol h^{-1}. Conversion of H_2 in the reactors is 46.67 % while the overall conversion of H_2 is 76.67 %. About 33.90 % of the wax is produced in the first FT reactor. The amount of heat needed to be removed from the reactors to keep the reactor temperatures constant at 210 °C is 1.13×10^9 kJ h^{-1}. The amount of make-up natural gas to the fired heater is 1343 kmol h^{-1} which is 277 kmol h^{-1} less than in case 1. Here, 145 kmol h^{-1} of CO_2 is emitted to the atmosphere via purge stream.

3.4 Case with Four-Stage FT Reactors and Product Separation between Stages

In this case, the GTL process with four-stage FT reactors is optimized (n_s = 4). The results of optimization of this case are presented in Tab. 2 and are very close to the case with three-stage reactors.

Tab. 4 presents the selectivity of the liquid hydrocarbon stream leaving the three-phase separator (Fig. 2, to upgrading unit stream at 30 °C). This stream then goes through the upgrading section which is not considered here. It is important to note that light hydrocarbons (Fig. 2, light ends stream at 30 °C) are recycled back to the process. This stream contains mainly CO (62.13 %), H_2 (20.50 %), CO_2 (9.19 %), CH_4 (2.43 %), and the rest consists of N_2 and other hydrocarbons on mole basis (single-stage FT reactor). The weight fraction of C_{21+} is about 85 % of the final product.

Staging of cobalt-based FT reactors was studied by Rafiee and Hillestad. They used lumping of components to reduce the number of components. Staging of the FT reactor will increase the production rate of key components [20, 21]. Maretto and Krishna optimized a multistage slurry bubble column reactor for FTS [12]. The results demonstrate that staging of the reactor increases syngas conversion and reactor productivity.

A case study is carried out to assess the impact of reactor staging at constant conversion. The wax production rate of a two-stage FT configuration is set at 77 753 kg h^{-1}, i.e., the same

Table 4. Carbon distribution of liquid hydrocarbon product.

	Selectivity [%]					
n_s	C_1	C_2	C_3–C_4	C_5–C_{10}	C_{11}–C_{20}	C_{21+}
1	0.015	0.001	0.023	3.144	11.405	85.411
2	0.020	0.001	0.031	3.391	11.759	84.798
3	0.021	0.001	0.034	3.533	12.071	84.339
4	0.021	0.001	0.034	3.544	12.092	84.307

production rate as a single-stage reactor. In this case, the required volume is 1950 m^3 and the volume reduction compared to the single-stage reactor is 50 m^3.

4 Conclusions

A novel design of a GTL process with a multistage cobalt-based FT reactor and interstage product separation is presented. The kinetic model is the one given by Iglesia. The objective function is maximization of wax (C_{21+}) at the end of the reactor path. The degrees of freedom include the steam-to-hydrocarbon ratio (S/C) to the prereformer, the oxygen-to-hydrocarbon ratio (O/C) to the ATR, the tail gas purge ratio, the recycle tail gas fraction to the syngas and FT sections, the CO_2 removal fraction, and the number of stages.

The results indicate that the production rates of wax for a single-, two-, and three-stage FT reactor of the same total volume of 2000 m^3 are 77 753, 78 948, and 79 216 kg h^{-1}, respectively.

The authors have declared no conflict of interest.

Symbols used

k_1	[$kmol_{CH4} Pa^{-1.05} m^{-3}_{reactor} s^{-1}$]	kinetic parameter
k_2	[$kmol_{CO} Pa^{-1.25} m^{-3}_{reactor} s^{-1}$]	kinetic parameter
K_1	[Pa^{-1}]	adsorption parameter
n	[–]	carbon number
n_s	[–]	number of stages
P_{CO}	[Pa]	partial pressure of CO
P_{H2}	[Pa]	partial pressure of H_2
r_{CH4}	[$kmol_{CH4} m^{-3}_{reactor} s^{-1}$]	production rate of CH_4
r_{CO}	[$kmol_{CO} m^{-3}_{reactor} s^{-1}$]	consumption rate of CH_4
U_{H2}	[–]	usage ratio of H_2
V_i	[m^3]	volume of each stage
W_n	[–]	mass fraction of C_n, n = 2, 3,…

Greek letter

α	[–]	chain growth probability

Abbreviations

ASF	Anderson-Schulz-Flory
ASU	air separation unit
ATR	auto-thermal reforming
BFW	boiler feed water
CSTR	continuous stirred-tank reactor
FT	Fischer-Tropsch
FTS	Fischer-Tropsch synthesis
GHR	gas-heated reforming
GTL	gas-to-liquid
O/C	oxygen-to-hydrocarbon ratio
OCM	oxidative coupling of methane
S/C	steam-to-hydrocarbon ratio
SBCR	slurry bubble column reactors
SMDS	Shell middle distillate synthesis
SMR	steam methane reforming

References

[1] M. E. Dry, A. P. Steynberg, *Fischer-Tropsch Technology*, 1st ed., Elsevier, Amsterdam **2004**.

[2] J. Rostrup-Nielsen, I. Dybkjaer, K. Aasberg-Petersen, *Fuel Energy Abstr.* **2002**, *43 (1)*, 38. DOI: 10.1016/S0140-6701(02)80388-5

[3] A. de Klerk, E. Furimsky, *Catalysis in the Refining of Fischer-Tropsch Syncrude*, 1st ed., RSC Publishing, Cambridge, UK **2010**.

[4] K. Aasberg-Petersen, T. S. Christensen, C. Stub Nielsen, I. Dybkjær, *Fuel Process. Technol.* **2003**, *83 (1)*, 253–261. DOI: 10.1016/S0378-3820(03)00073-0

[5] P. K. Bakkerud, *Catal. Today* **2005**, *106 (1)*, 30–33. DOI: 10.1016/j.cattod.2005.07.147

[6] https://en.wikipedia.org/wiki/Fischer%E2%80%93Tropsch_process (Accessed on January 20, 2016)

[7] GTL-Workshop, *Introduction to GTL Technology*, Pre-Symposium Workshop, Gas Processing Center and Shell Co., Doha, Qatar **2010**.

[8] www.shell.com/about-us/major-projects/pearl-gtl.html (Accessed on January 20, 2016)

[9] M. Panahi, A. Rafiee, S. Skogestad, M. Hillestad, *Ind. Eng. Chem. Res.* **2012**, *51*, 425–433. DOI: 10.1021/ie2014058

[10] I. P. Androulakis, S. C. Reyes, *AIChE J.* **1999**, *45*, 860–868. DOI: 10.1002/aic.690450417

[11] V. Diakov, A. Varma, *Ind. Eng. Chem. Res.* **2003**, *43 (2)*, 309–314. DOI: 10.1021/ie0208624

[12] C. Maretto, R. Krishna, *Catal. Today* **2001**, *66*, 241–248. DOI: 10.1016/S0920-5861(00)00626-X

[13] T. Waku, S. Y. Yu, E. Iglesia, *Ind. Eng. Chem. Res.* **2003**, *42*, 3680–3689. DOI: 10.1021/ie030255w

[14] S. Hwang, R. Smith, *Chem. Eng. Sci.* **2004**, *59*, 4229–4243. DOI: 10.1016/j.ces.2004.05.037

[15] L. Guillou, S. Paul, V. L. Courtis, *Chem. Eng. J.* **2008**, *136*, 66–76. DOI: 10.1016/j.cej.2007.03.030

[16] F. Stuber, H. Delmas, *I&EC* **2003**, *42*, 6–13. DOI: 10.1021/ie020466l

[17] T. Ngwenya, D. Glasser, D. Hildebrandt, N. Coville, P. Mukoma, *I&EC* **2005**, *44*, 5987–5994. DOI: 10.1021/ie0493199

[18] F. Manenti, A. R. Leon-Garzon, Z. Ravaghi-Ardebili, C. Pirola, *Appl. Therm. Eng.* **2014**, *70*, 1228–1237. DOI: 10.1016/j.applthermaleng.2014.04.011

[19] M. Hillestad, *Chem. Eng. Sci.* **2010**, *65*, 3301–3312. DOI: 10.1016/j.ces.2010.02.021

[20] A. Rafiee, M. Hillestad, *Comput. Chem. Eng.* **2012**, *39*, 75–83. DOI: 10.1016/j.compchemeng.2011.11.009

[21] A. Rafiee, M. Hillestad, *Chem. Eng. Technol.* **2013**, *36*, 1729–1738. DOI: 10.1002/ceat.201200700

[22] T. S. Christensen, *Appl. Catal., A* **1996**, *138 (2)*, 285–309. DOI: 10.1016/0926-860X(95)00302-9

[23] K. Aasberg-Petersen, J. H. Bak Hansen, T. S. Christensen, I. Dybkjaer, P. S. Christensen, C. Stub Nielsen, S. E. L. Winter Madsen, J. R. Rostrup-Nielsen, *Appl. Catal., A* **2001**, *221*, 379–387. DOI: 10.1016/S0926-860X(01)00811-0

[24] I. C. Yates, C. N. Satterfield, *Energy Fuels* **1991**, *5 (1)*, 168–173. DOI: 10.1021/ef00025a029

[25] E. Iglesia, S. C. Reyes, S. L. Soled, *Computer-Aided Design of Catalysts*, 1st ed., Marcel Dekker, New York **1993**.

[26] S. T. Sie, *Rev. Chem. Eng.* **1998**, *14*, 109–157. DOI: 10.1515/REVCE.1998.14.2.109

